J|A|C|S
ARTICLES
Published on Web 07/12/2006

SHARP-TACSY: Triple-Band Tailored Correlated Spectroscopy for Base-to-Sugar Transfer in Nucleic Acid Residues with Intermediate Time Scale Motions

Christophe Farès and Teresa Carlomagno*

Contribution from the Max-Planck-Institute for Biophysical Chemistry, Department of NMR-Based Structural Biology, Am Fassberg 11, D-37077 Göttingen, Germany

Received March 9, 2006; E-mail: taco@nmr.mpibpc.mpg.de

Abstract: Established experiments to identify the sugar-to-base connectivity in isotopically labeled RNA require long transfer periods and are inefficient for residues undergoing intermediate time scale motions (microsecond to millisecond). Here, an alternative transfer experiment is introduced, whereby the C1′−N1/9−C6/8 spin system is selectively brought to the so-called Hartmann−Hahn condition using *selective heteronuclear planar triple-band tailored correlated spectroscopy* (SHARP-TACSY). Results are shown for the fully labeled 30-mer oligonucleotide TAR RNA with particular attention placed on residues from and close to the bulge and the loop. For these residues, the faster relaxation can be attributed to exchange contributions stemming from transient stacking and unstacking of the bases and/or from the isomerization of the ribose sugar pucker. The new experiment shows improved signal-to-noise for residues exhibiting large microsecond−millisecond time scale motions with respect to established experiments, thus providing a valid alternative for resonance assignment in mobile RNA regions.

Introduction

The identification of the sugar-to-base correlation in isotopically labeled RNA and DNA is one of the most important and challenging steps toward the NMR assignment of oligonucleotide resonances. Commonly used are experiments which correlate the C1′/H1′ group of the sugar moiety with the C8/H8 (C6/H6) group of the purine (pyrimidine) ring, using their scalar coupling to the intervening N9 (N1) as the magnetization transfer mechanism. Despite the necessary long evolution periods (80−100 ms), these transfers have been optimized to partially overcome the relaxation problems associated with large systems.[1−4] The most notable of these experiments are the relaxation-optimized triple-resonance out-and-back $H^{s/b}CN$ and all-the-way-through $H^{s}CNCH^{b}$ experiments, making use of multiple quantum coherence transfer (MQ) in the sugar (superscript "s") and/or the TROSY interference effect (TR) in the base (superscript "b") as described by Sklenář et al.[4] and Fiala et al.[1] In all cases, these coherence transfers take place under the effect of the B_0 field (laboratory frame) and are particularly prone to exchange broadening due to motions causing chemical shift changes $\Delta\delta$ on a time scale nearing $\tau_{ex} = \Delta\delta^{-1}$ (usually in the ms-μs time range). Indeed, the sensitivity of these experiments is severely impeded for residues undergoing motions, such as sugar pucker isomerization or base-ring movements, in this time regime. Such structural fluctuations are more commonly observed in the non-canonical elements of RNA structure (such as turns, bulges and loops) rather than in the stable helical stems. Consequently, the intrinsic dynamics often seen in the functionally relevant RNA structure elements seriously complicates the basic NMR assignment procedure, especially in larger systems.

Here, an alternative experiment is introduced in which a base-to-sugar transfer is accomplished in a single step by bringing the C1′−N1/9−C6/8 spin system to the so-called Hartman−Hahn condition.[5,6] In the rotating frame, microsecond-to-millisecond chemical shift exchanges within the irradiated bands do not contribute to the relaxation. The C1′−N1/9−C6/8 spin system is uniquely suited for rotating frame coherence transfer because of its quasi-symmetric coupling topology ($^1J_{C1'\,N1/9} = 11-12$, $^1J_{C6/8\,N1/9} = 11-12$, $^2J_{C1'\,C6/8} = 0$ Hz), which allows nearly complete transfer of the magnetization from one carbon to the other after $(\sqrt{2}\,^1J)^{-1} \sim 118$ ms mixing, neglecting relaxation.[7] Therefore, in the new experiment, the efficiency of magnetization transfer for residues undergoing intermediate time scale motions is not diminished by the large exchange-derived relaxation term active during the J-transfer steps of traditional experiments. The idea of utilizing rotating frame coherence transfer to suppress chemical shift exchange contributions to the relaxation has been previously used in the C'/C_α and C_β/C_{aro} correlations in protein backbone and side chains, respectively, where irradiation was applied on two well-separated ^{13}C regions.[8] The new experiment, applied to three spins on two

(1) Fiala, R.; Czernek, J.; Sklenář, V. *J. Biomol. NMR* **2000**, *16*, 291−302.
(2) Fiala, R.; Jiang, F.; Sklenář, V. *J. Biomol. NMR* **1998**, *12*, 373−383.
(3) Marino, J. P.; Diener, J. L.; Moore, P. B.; Griesinger, C. *J. Am. Chem. Soc.* **1997**, *119*, 7361−7366.
(4) Sklenář, V.; Dieckmann, T.; Butcher, S. E.; Feigon, J. *J. Magn. Reson.* **1998**, *130*, 119−124.
(5) Glaser, S. J.; Quant, J. J. In *Advances in Magnetic and Optical Resonance*; Warren, W. S., Ed.; Academic Press: San Diego, 1996; Vol. 19, pp 59−252.
(6) Zuiderweg, E. R. P.; Zeng, L.; Brutscher, B.; Morshauser, R. C. *J. Biomol. NMR* **1996**, *8*, 147−160.
(7) Schedletzky, O.; Luy, B.; Glaser, S. J. *J. Magn. Reson.* **1998**, *130*, 27−32.
(8) Carlomagno, T.; Maurer, M.; Sattler, M.; Schwendinger, M. G.; Glaser, S. J.; Griesinger, C. *J. Biomol. NMR* **1996**, *8*, 161−170.

10.1021/ja061424h CCC: $33.50

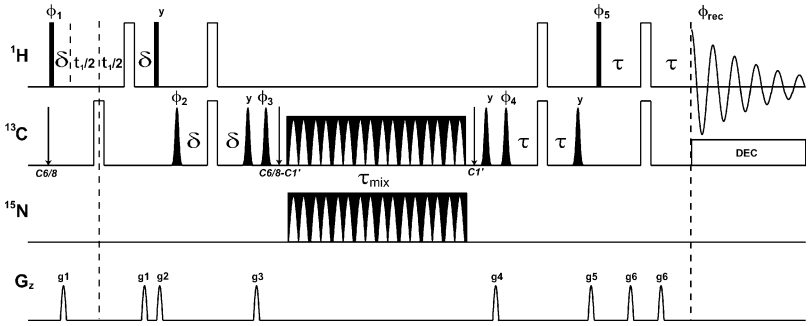

Figure 1. Pulse sequence for the SHARP-TACSY (H^bCNCH^s) experiment. Filled and open pulse symbols represent $\pi/2$ and π rf pulses. The shaped pulses symbolize selective Gaussian cascade Q5 excitation pulses. All pulse phases are along x except where otherwise indicated. Phase cycling consists of $\phi_1 = x, -x, \phi_2 = 2(x), 2(-x), \phi_3 = 4(y), 4(-y), \phi_4 = 8(x), 8(-x), \phi_5 = 16(x), 16(-x), \phi_{rec} = abba$, where $a = (x, -x, -x, x)$ and $b = (-x, x, x, -x)$. Long shaded pulses indicate the rf-matched selective pulse train (with MLEV16 supercycle) for TACSY transfer. Transfer delays are $\delta = 1.25$ ms and $\tau = 1.5$ ms. Arrows indicate ^{13}C carrier frequency switches. The gradient intensities used for $g1$, $g2$, $g3$, $g4$, $g6$ were 21, 30, 24, 35, 17, and 8 G/cm, respectively.

channels, is called *selective heteronuclear planar triple-band tailored correlated spectroscopy* (SHARP-TACSY).

Materials and Methods

Sample Preparation. The uniformly labeled 30-mer oligonucleotide encompassing the transactivation response (TAR) element of HIV-2 RNA (^{16}GGCCAGA^{23}U^{25}UGAGCCUGG-GAGCUCUCUGGC^{46}C) was enzymatically synthesized from labeled NTPs as described previously.[9] The RNA was dissolved in buffer with D_2O (99.95%), heated to 80 °C for 2 min, allowed to anneal at 0 °C for 2 min, and transferred to a Shigemi sample tube. The total sample volume was 250 μL for a final concentration of 0.5 mM. All experiments were performed maintaining the sample temperature at 298 K.

NMR Spectroscopy. The 2D SHARP-TACSY (H^bCNCH^s) pulse sequence is shown in Figure 1. The key element of the pulse program is the central "tailored" triple-band irradiation during which the three nuclei, C1′, C6/8, and N1/9, are mixed under the effect of a planar coupling Hamiltonian in the rotating frame, giving rise to the desired single-quantum coherence transfer from C6/8 to C1′. By virtue of a selective pulse train on the ^{13}C channel, modulated by $\cos(\pi\Delta\nu t)$, the two bands corresponding to the C1′ and C6/8 chemical shift ranges and separated by $\Delta\nu$ can be simultaneously irradiated. Concurrently, the N1/9 is irradiated by applying a frequency-matched nonmodulated pulse train on the ^{15}N channel. The constituent pulse element, a smoothed double 270° Gaussian pulse with 15% truncation (G2s), was designed to optimize transfer efficiency over the selected bands while minimizing band interference. The calculations which lead to the design and choice of the G2s pulse are discussed below. The pulse train is expanded with the MLEV-16 supercycle and repeated to match the desired mixing time. The mixing pulse train is flanked by two selective double $^1H-^{13}C$ INEPT steps, using Q5 excitation pulses to ensure that the transfer occurs exclusively from the base to the sugar. Thus, the first double INEPT prepares the incoming transverse C6/8 magnetization, and the second transforms the out-coming transverse C1′ magnetization into H1′ for detection. An indirect evolution t_1 is introduced on H6/8. The direction of the transfer can be inverted by reversing the sequence of carrier frequency switches on the ^{13}C channel. An additional indirect dimension can be placed on the carbon channel prior to the mixing, as proposed for the PLUSH-TACSY experiment.[8] For added resolution or for ease of assignment in 2D, one can effectively filter for purines or for pyrimidines by simply setting the ^{15}N carrier frequency on the N9 or N1 chemical shift, thus avoiding the necessity to resort to alternate labeling schemes.

Also of importance is the rf power requirement during the full 118 ms mixing time. Although the peak intensity during the irradiation reaches 6 and 3 kHz on the ^{13}C and ^{15}N channels, the average power applied corresponds to continuous irradiation at 2 and 1 kHz, respectively, equivalent to simultaneous decoupling schemes commonly applied on carbon and nitrogen for triple-resonance experiments on biomolecules. This new experiment can thus easily be implemented on most commercial spectrometers and probe heads including actively cooled systems for sensitivity enhancement.

The 2D SHARP-TACSY (H^bCNCH^s) was performed either on all residues or selectively targeting separately the pyrimidines (U/C) or the purines (A/G) residues of a simple NTP mixture or of the 30nt-TAR RNA. Delay, phase, and gradient details are described in the Figure 1 captions. For comparison of the transfer efficiency, a 2D MQ/TR$-H^sCNCH^b$ experiment was set up as described by Fiala et al.[1] but placing the indirect dimension on the ^1H rather than on ^{15}N and using exactly the same number of scans and increments as for the 2D SHARP-TACSY (H^bCNCH^s). All experiments were implemented on a Bruker Avance spectrometer operating at 14.1 T using a triple-resonance $^1H/^{13}C/^{15}N$ probehead equipped with z-gradient shim coils.

Simulation of Selective Irradiation. To optimize the magnetization transfer efficiency of the triple-band irradiation in the SHARP-TACSY experiment, the effects of different pulse trains on the RNA spin system of interest were simulated. A script written in Γ ("Gamma") language (version 4.1.0)[10] was utilized to calculate coherence evolution curves and offset profiles for typical RNA spin systems under the triple-band irradiation condition as a function of the pulse shape profile. Two shapes were used for these simulations: G2, a 540° pulse consisting of two back-to-back Gaussian curves with 15% truncation level (Figure 2A), and G2s, a 540° pulse obtained by coadding two half-Gaussian curves overlapping at their 15% level (Figure 2B). The program determined the evolution of a three- or four-spin system (e.g., C6/8−N1/9−C1′ or C5−C6−

(9) Milligan, J. F.; Groebe, D. R.; Witherell, G. W.; Uhlenbeck, O. C. *Nucleic Acids Res.* **1987**, *15*, 8783−8798.

(10) Smith, S. A.; Levante, T. O.; Meier, B. H.; Ernst, R. R. *J. Magn. Reson., Ser. A* **1994**, *106*, 75−105.

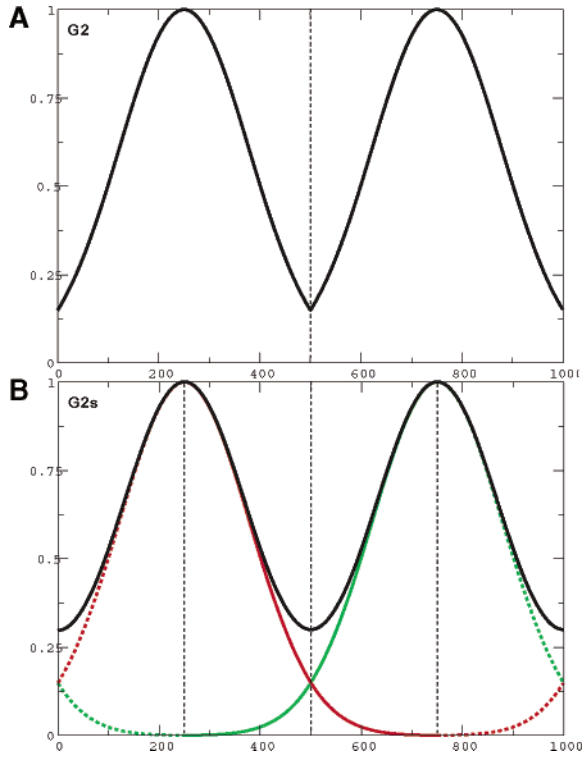

Figure 2. (A) G2 shape (black line) is constructed by concatenating two Gaussian functions truncated at 15%. (B) The "smoothed" G2s (black line) was obtained by coadding two half-Gaussian functions intersecting at their 15% level (green and red lines).

N1−C1′) under the influence of individual propagators corresponding to short rectangular rf elements that trace the pulse shape intensity and phase profile for the entire mixing sequence. The spin systems were defined by their isotropic chemical shift and weak scalar coupling according to the range of values given in Table S1 (Supporting Information). The 2D offset profiles were typically evaluated by determining the transfer efficiency from C6/8 to C1′ using a grid of 50 × 50 different offset pairs, thus mapping a 2000 Hz × 2000 Hz area. Details of the other relevant simulation parameters are indicated in the respective figure captions.

Theory

Relaxation Rate: SHARP-TACSY versus MQ/TR HCNCH. To accurately compare the effect of R_1 and R_2 relaxation during the established (MQ/TR) and new experiment (SHARP-TACSY) in the absence of intermediate time scale motions, a theoretical description of the active relaxation rates is presented here. The dominant relaxation processes in the MQ/TR−H^{s}CNCH^b experiment occur during the MQ transfer $H_y{}^sC_x{}^s \rightarrow C_y{}^sN_z{}^b$ and the sensitivity-optimized SQ transfer $N_z{}^bC_y{}^b \rightarrow C_y{}^bH_z{}^b$, for total delays of 30 and 28.75 ms, respectively. With the use of a simple isotropic diffusion model and the theoretical relaxation rates $R_2{}^{MQ}$ and $R_2{}^{TR}$ from Fiala et al.[1] (but using B_0 = 14.1 T, τ_c = 4 ns), these relaxation mechanisms would be responsible for a total intensity loss of 40−50%. The range depends on residue type, on the presence of rapid internal motions ($\tau_e \ll 4$ ns, $S^2 = 0.75-1.00$), and/or on the presence of a neighboring ^{1}H nucleus.

Under the planar mixing of SHARP-TACSY, the average Hamiltonian for the three spin $^1/_2$ system can be written as

$$H_{\text{eff}} = 2\pi J_{C^bN^b}(C_y{}^bN_y{}^b + C_z{}^bN_z{}^b) + 2\pi J_{N^bC^s}(N_y{}^bC_y{}^s + N_z{}^bC_z{}^s) \quad (1)$$

where the $C^b-N^{b-}C^s$ spin system corresponds to the pyrimidine C6−N1−C1′ spin system or the purine C8−N9−C1′ spin system. Under this Hamiltonian, the interconverting coherences present during the irradiation are

$$C_x{}^b,\ N_x{}^b,\ C_x{}^s,\ 2C_y{}^bN_z{}^b,\ 2C_z{}^bN_y{}^b,\ 2N_y{}^bC_z{}^s,\ 2N_z{}^bC_y{}^s,\ 4C_y{}^bN_x{}^bC_y{}^s,\ 4C_z{}^bN_x{}^bC_z{}^s$$

The overall relaxation taking place during the transfer $C_x{}^b \rightarrow C_x{}^s$ thus involves all of these terms, as described by Majumdar and Zuiderweg.[11] As estimated by numerically solving the relaxation matrix (eqs 74 and 75 from Majumdar and Zuiderweg[11]), it is found that the overall signal loss during the magnetization transfer from $C_x{}^b$ to $C_x{}^s$, assuming perfectly symmetric scalar coupling topology, would be approximately 10−20%, depending as above on the presence of motions and/or neighboring ^{1}H nuclei. The ^{13}C single-quantum transverse relaxation rates were also predicted as in Fiala et al.[1] The relaxations of the ^{15}N single-quantum and triple-quantum terms were estimated to be 5 and 100 s^{-1}, although the transfer efficiencies were less sensitive to these.

When the relaxation in both experiments are compared, the SHARP-TACSY experiment is expected to deliver 25−40% signal with respect to the relaxation-optimized MQ/TR−H^{s}CNCH^b experiment for oligonucleotides of the size of TAR RNA in the absence of intermediate (microsecond−millisecond) time scale motions. These numbers clearly do not forecast a good performance of the new experiment; however, for cases where intermediate time scale motions causing chemical shift exchanges are present, larger R_2 rates are anticipated for the MQ/TR−H^{s}CNCH^b experiment, whereas the relaxation rates in the TACSY experiment are unperturbed. In those cases, a higher SN_{TACSY}/SN_{MQTR} ratio is expected. In the likely cases where the exchange correlation time τ_{ex} approaches $(\Delta\delta)^{-1}$, the TACSY efficiency exceeds that of the MQ/TR counterpart. For example, an exchange relaxation term due to equally populated two-site jump causing a carbon chemical shift change of 300 Hz (2 ppm at 14.1 T) at a rate in a range between 10^4 to 10^3 s^{-1} would contribute additional relaxation on the order of 10^0 to 10^1 s^{-1}. These numbers are of the same magnitude as the $R_2{}^{MQ}$ and $R_2{}^{TR}$ expected for a rigid molecule and thus would contribute to the decrease of the S/N by a factor of up to 2−3 in the MQ/TR. As a result, the SHARP-TACSY would be more sensitive. Exchange terms of this order have been directly measured in RNA, including TAR and the cUUCGg tetraloop motif.[12]

Results and Discussion

Constituent Pulse Design: G2 versus G2s. In the choice of the constituent pulse element R for the ^{13}C double-band, ^{15}N single-band irradiation of the SHARP-TACSY sequence, the following conditions have to be fulfilled to achieve the desired three-spin effective planar coupling Hamiltonian defined in eq 1. (i) First, the number of modulation cycles n must be an integer

(11) Majumdar, A.; Zuiderweg, E. R. P. *J. Magn. Reson., Ser. A* **1995**, *113*, 19−31.
(12) Duchardt, E.; Schwalbe, H. *J. Biomol. NMR* **2005**, *32*, 295−308.

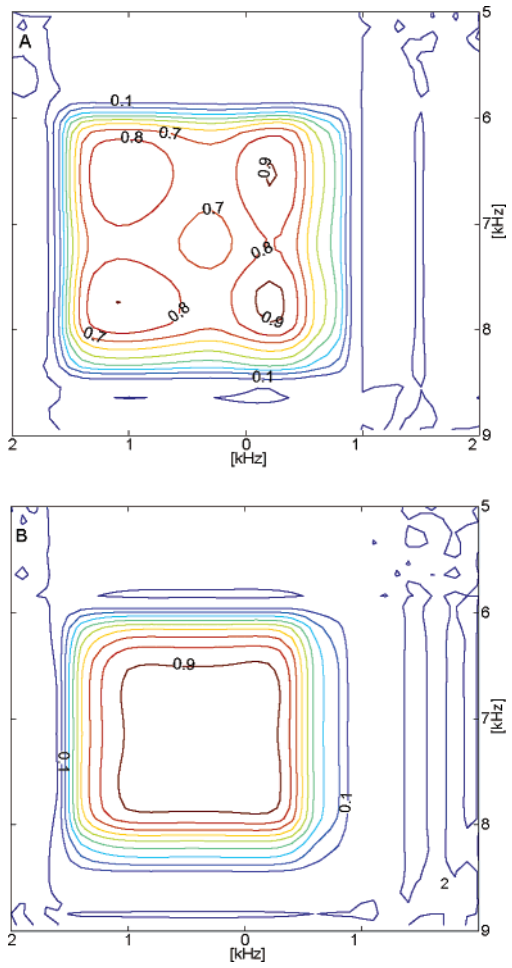

Figure 3. Offset profile of the transfer efficiency for shapes (A) G2 and (B) G2s, simulated using a program written in Γ language (version 4.1.0) (ref 10). Shape parameters included $n = 6$, $\Delta\nu = 7545$ Hz, $B_0 = 14.1$ T, $\tau_R = 795$ μs, $\nu_{max} = 6201$ Hz (G2), and $\nu_{max} = 5891$ Hz (G2s). Pulse trains were expanded to an MLEV16 supercycle and repeated 10 times for a total mixing of 127ms. Scalar couplings of $^1J_{C6,N1} = 12$ and $^1J_{N1,C1'} = 12$ Hz were used.

multiple of $\Delta\nu^{-1}$ so that the three individual rotating frames coincide at the end of the duration of R ($\tau_R = n\Delta\nu^{-1}$); this ensures that the effective rf Hamiltonian is equivalent for all three spins. (ii) Second, the excitation bands must be well separated to avoid mutual interference and to allow the two ^{13}C to be considered as pseudoheteronuclei ($\Delta\nu \gg \nu_1^{max}$). (iii) Third, the shaped inversion pulse must be symmetric and purely amplitude-modulated ($\varphi = 0$ or π) such that the three operator trajectories spend time equally along the *z*- and *y*-axis and evolve exclusively in the *yz*-plane. Additional shape requirements are exclusive to chemical shift ranges of nucleotides (Table S1). The carbon double-selective bandwidths ($\Delta\nu_b$) must cover the C6/8 and C1′ chemical shift ranges (131−144 ppm and 87−94 ppm), while the nitrogen selective band must cover the N1/9 chemical shift range (142−172).

The G2 element (Figure 2A) satisfies conditions (i) and (iii).[8] The two ^{13}C bands for the C1′−C6/8 of nucleic acids ($\Delta\nu = 8$ kHz, $\nu_1^{max} = 6$ kHz) are prone to cross-band interference (condition (ii)), as can be appreciated in the simulated offset profile in Figure 3A. The contour plot shows the transfer efficiency as a function of incoming C6/8 frequency (centered at 0 Hz, horizontal scale) and out-coming C1′ frequency (centered at 7545 Hz, vertical scale). The use of the G2 element has severe drawbacks, such as an asymmetric extension of the two selective bands toward each other and a large dependence of the transfer efficiency on the chemical shift within the irradiation bands. Softening the sharp edges of the G2 element, such as in the G2s (Figure 2B), significantly alleviates the problems stemming from field inhomogeneities. As can be appreciated in Figure 3B, a homogeneous high transfer efficiency (>0.9) is reached over a square area of 1.5 kHz in both dimensions for similar conditions. The difference in transfer efficiency between the two shapes was verified on a simple sample composed of a mixture of NTPs (see below).

Since the cross-band interference skews both the size and position of the selection area, simulations were performed for several sets of parameters that would result in effective homogeneous transfer efficiency over two carbon bands of 7−14 ppm separated by 40−52 ppm. The results are summarized in Table S2 of the Supporting Information for four different static magnetic field strengths (600−900 MHz) and can be used as a guide for choosing convenient shape parameter for a given RNA sample. In general, the one-sided 50% extension of the excitation bands toward each other can be corrected for by increasing both $\Delta\nu$ and ν_1^{max}. For the general application of SHARP-TACSY to RNA, one should exceed the center-to-center band separation by about 10% and adjust the power level accordingly.

Influence of Passive Spin Coupling. In uniformly labeled nucleotides, the presence of other carbon nuclei with a nonzero scalar coupling to the C6/8−N1/9−C1′ spin system can have a large deleterious effect on the transfer efficiency of the SHARP-TACSY, if they are not properly excluded from the irradiation bands. These passive spin couplings originate from the C2′ and the C4′ of the ribose, the C5 of the pyrimidine base, and the N3 of the guanine base (Table S1). The effect of these neighboring nuclei can also be easily simulated. The chemical shift range of the C4′ starts only 1 ppm upfield from the end of the C1′ range, but its scalar coupling to the C1′ is usually less than 2 Hz. Simulations show that its presence in the irradiation band affects transfer minimally (7%). The C2′ shares a larger scalar coupling (43 Hz) with C1′ and thus imposes a much more stringent upfield limit to the C1′ irradiation band.

The chemical shift range of the N9 of the guanine base overlaps perfectly with that of its N3 and can therefore not be decoupled through the selectivity of the shapes. As a result, the simulation expects a 15% reduction of the transfer efficiency for all guanine residues, assuming a 4 Hz coupling between the two ^{15}N nuclei. However, this reduction was not observed experimentally on the NTP sample (see below) which implies that the coupling reported by Buchner et al.[13] may have been overestimated.

The largest effect is expected for the C5 nucleus of the cytosine residues which has a substantial coupling to the C6 spin (57 Hz) and whose theoretical chemical shift range partially overlaps with that of C1′. The time evolutions of the magnetization transfer from C6 to C1′ are displayed in Figure 4 and were calculated using the G2s shape and parameters described in Figure 3B. Three cases are shown where the C5 chemical shift coincides with the transfer efficiency contour line of 0.9 (A, 93 ppm), 0.1 (B, 100 ppm), and 0.0 (C, 108 ppm) (see the contour lines of Figure 2B). Because of its large scalar coupling to C6,

(13) Buchner, P.; Maurer, W.; Ruterjans, H. *J. Magn. Reson.* **1978**, *29*, 45−63.

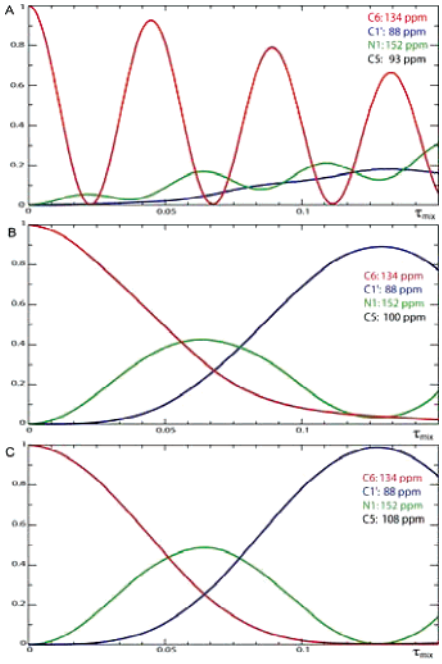

Figure 4. Effect of pyrimidine C5 chemical shift and interference of the $^1J_{C5,C6}$ coupling on transfer efficiency. The time evolutions of the rotating frame longitudinal magnetizations for the pyrimidine four-spin system C5−C6−N1−C1′ under continuous planar mixing, starting with 100% $C6_x$ (red), 0% $N1_x$ (green), and 0% $C1'_x$ (blue) is shown. The simulations used parameters $n = 6$, $\Delta\nu = 7545$ Hz, $B_0 = 14.1$ T, $\tau_R = 795$ μs, $\nu_{max} = 5891$ Hz, carrier frequency = 113 ppm, and shape G2s. Also assumed are $^1J_{C5,C6} = 57$, $^1J_{C6,N1} = 12$, and $^1J_{N1,C1'} = 12$ Hz. The chemical shifts for C6 and C1′ are kept at 134 and 88 ppm, respectively, while C5 is set to 93 ppm (A), 100 ppm (B), and 108 ppm (C).

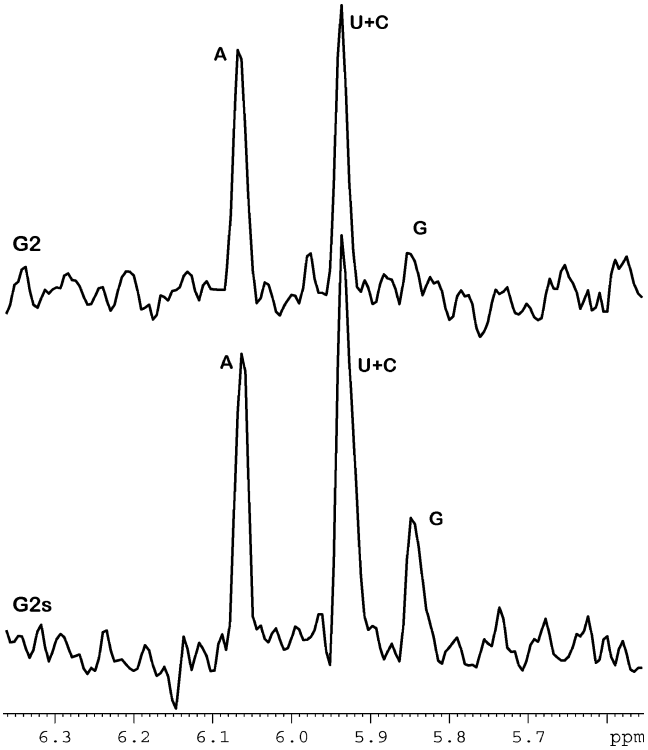

Figure 5. 1D projection spectrum (64 transients) of SHARP-TACSY (H^b-$CNCH^s$) applied to a mixture of ATP/CTP/UTP/GTP using pulse elements G2 (top) and G2s (bottom) during the 121 ms irradiation mixing. Shape parameters included $n = 8$, $\Delta\nu = 9684$ Hz, $B_0 = 16.4$ T, $\tau_R = 841.3$ μs, $\nu_{max} = 5860$ Hz (G2), and $\nu_{max} = 5567$ Hz (G2s).

the C5 nuclei which are most shifted toward high field, thus entering the irradiation band, have an important truncation effect on the transfer efficiency to C1′. It is thus essential to carefully position the bands to reduce the effect of passive coupling to the C5. In most cases, the steepness of the G2s selection band is sufficient to include all C1′ and exclude all C5 from the irradiation band, except on rare occasions where the cytosine C5 resonate lower than about 97 ppm.

SHARP-TACSY Transfer Efficiency for the NTPs Mixture. The difference in transfer inhomogeneities of the modulated G2 and G2s bands was reproduced on a simple uniformly labeled NTP sample consisting of ATP, GTP, UTP, and CTP. Figure 5 compares the 1D projections of SHARP-TACSY using equivalent mixing sequences ($n = 8$, $\Delta\nu = 9684$ Hz, $B_0 = 16.4$ T) for G2 and G2s on the same sample. Whereas the ATP cross-peak is almost equivalent in both experiments, the G2 shape yielded only 70% of the CTP and UTP cross-peak intensities, while the transfer for the GTP was almost completely suppressed compared to that of the G2s. On the other hand, the cross-peak intensity ratio in the G2s experiment reflects approximately the NTP concentration ratio present in the sample, demonstrating the excellent homogeneous transfer efficiency within the irradiation bands and the proper exclusion of the C5′ chemical shift of CTP.

SHARP-TACSY Transfer Efficiency for the TAR−RNA. The challenge in achieving base-to-sugar correlation in elongated nucleic acids lies in the two CN transfer steps which rely on the evolution of their small 11−12 Hz coupling, during which transverse relaxation is active. The faster relaxation associated with the slower correlation times of larger systems has been circumvented with the development of optimized experiments making use of MQ and TROSY transfers; however, the relaxation mechanism due to intermediate time scale motions is still active. To avoid microsecond−millisecond exchange-induced relaxation, a rotating frame transfer can replace the conventional INEPT at the cost of a longer overall transfer duration. For example in a two spin $^1/_2$ system using a double-band heteronuclear planar mixing experiments, the transfer delay is generally longer by a factor 2 relative to that of the single INEPT step. To this effect, a small gain is obtained moving to a symmetric three spin $^1/_2$ system ($J_{12} = J_{23}$), since the mixing duration of the triple-band planar mixing experiment only exceeds the double INEPT by a factor of $\sqrt{2}$ (it is reduced by a factor of $\sqrt{2}$ compared to two back-to-back double-band mixing sequences). It is clear that moving to rotating frame transfers only makes sense when signal gain due to intermediate time scale motion exceeds the signal loss due to the longer mixing time.

To demonstrate the importance of intermediate time scale motions in large RNA and that the resulting signal loss can be partially retrieved using a Hartman−Hahn transfer instead of an INEPT transfer, both the MQ/TR H^sCNCH^b and the SHARP-TACSY H^bCNCH^s experiments were performed for the same number of scans and increment on the same TAR RNA sample (Figure 6). The signal-to-noise ratio was measured for all well-resolved cross-peaks in both experiments and compared as a residue-specific relative ratio (SN_{TACSY}/SN_{MQTR}) in Figure 7. As described in the Theory section, in the absence of chemical exchange broadening, one anticipates the signal of the rotating frame experiments to be lower by a factor of 0.25−0.40, considering the active transverse relaxation during the total

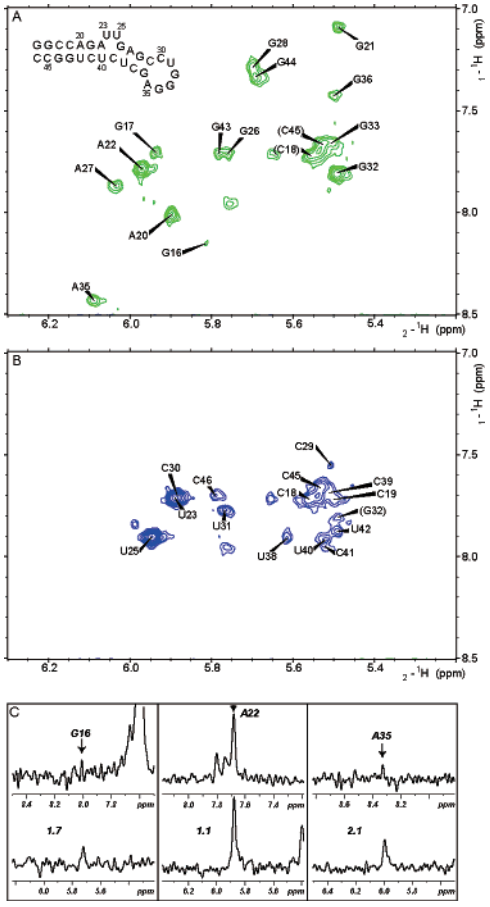

Figure 6. (A and B) 2D H6/8−H1′ correlation spectra recorded at 14.1 T using the SHARP-TACSY (H^bCNCH^s) on a 0.5 mM TAR RNA/D_2O sample at 298 K. Spectra (192 transients, 128 increments) were acquired separately with the ^{15}N carrier optimized for purines (A/G) at 168 ppm (A) or for pyrimidines (C/U) at 152 ppm (B). The spectral widths were 2 and 10 ppm in the indirect and direct dimensions, respectively. The G2s pulse element was used ($\tau_R = 795\ \mu s$, $n = 6$, $\Delta\nu = 50$ ppm, and $\nu_1^{max} = 6201.2$ Hz (^{13}C) and 3100.6 Hz (^{15}N)). (C) Comparison of the direct dimension traces for three residues (G16, A22, A35) from the SHARP-TACSY−H^s-$CNCH^b$ (bottom) and MQ/TR−H^sCNCH^b (top). The latter experiment was acquired as described by Fiala et al. (ref 1). Numbers correspond to the ratio of S/N, measured from the cross-peak volume over a boxed area corresponding to twice the full-width at half-height in both dimensions.

transfer time for both experiments (94 ms for the MQ/TR−H^s-$CNCH^b$ vs 118 ms for TASCY). However, intermediate time scale structural fluctuations led to various levels of signal broadening and sensitivity loss in the MQ/TR−H^sCNCH^b experiment, which were avoided with the SHARP-TACSY experiment. Out of the 16 resolvable cross-peaks, the signal-to-noise ratio is better than expected for 11 residues. Many of these are concentrated around the flexible bulge region of TAR RNA and seem to indicate the presence of intermediate time scale motions. But, the real advantage of the new SHARP-TACSY experiment is seen for various residues located at the junction points between stem and loop regions. As displayed in Figures 6C and 7, the signals for three residues G16, A22, and A35 improve by a factor of 1.7, 1.1, and 2.2, respectively.

Several accounts on structure and dynamics in TAR RNA have reported a heterogeneous population of motions of different magnitude and over different time scales along the nucleic acid sequence. These studies have also shown the important contributions of intermediate time scale motions both in the nucleobase and ribose moieties.[14−17] Such motions have also been seen in many RNA molecules. For example, in the cUUCGg tetraloop motif, ^{13}C relaxation studies have concluded that intermediate time scale chemical exchange broadening was present for several residues, both in the ribose and base moieties, and concentrated around the loop as well as on the 3′ and 5′ terminal ends.[12]

For TAR−RNA, all important signal enhancements in the SHARP-TACSY experiment occur in nucleotides located at the junction between the mobile nonhelical elements and the more compact, relatively rigid stem elements. These signal gains show a good qualitative correlation with ^{13}C line widths, usually a good indicator that the base and sugar moieties of these residues present important intermediate time scale motions.

Residue G16, located at the free 5′-terminal end of the TAR RNA, is prone to undergo "fraying". Reports have demonstrated that base unpairing and unstacking requiring the breakage of H-bonds and of the favorable π-interactions occur more frequently at the terminal end of A-form helices and take place on the microsecond−millisecond time scale.[18] These motions are also evident from the breadth of the ^{13}C line widths of the C8 and C1′ measured in a 2D HSQC (data not shown). Interestingly, the same terminal base pair as here (G−C) located at the open end of the stem region of the 14-nt UUCG hairpin loop was shown to undergo large-scale chemical exchange motion.[12]

The A22−U40 base pair, which closes the lower stem at the bulge junction, is more dynamic than canonical A-form helix base pairs, as inferred from the fast solvent exchange rate of the U40 imino proton, whose NMR signal can only be observed at low temperature. The A22 site is an important recognition element for the Tat protein and Tat-derived peptides, and the flexibility of the A22 base might be of functional significance.[20−23] The ribose pucker of A22 also undergoes isomerization between the C3′-endo and C2′-endo conformations, as has been directly observed both from cross-correlated relaxation and scalar coupling parameters.[15,24,25]

Residue A35 is positioned at the 3′-end of the hexanucleotide apical loop, which has been found to be quite flexible in all NMR studies[26−28] with the ribose averaging between the C3′-endo and C2′-endo conformations. Both base stacking of A35 on G36 and of G34 on G36 was found to be consistent with structural restraints derived by NMR for a 14- and a 19-nucleotides hairpin containing the TAR hexanucleotide loop.[27,28]

(14) Dayie, K. T.; Brodsky, A. S.; Williamson, J. R. *J. Mol. Biol.* **2002**, *317*, 263−278.
(15) Hennig, M., The Scripps Research Institute, La Jolla, 2005, Private communication.
(16) Jaeger, J. A.; Tinoco, I. *Biochemistry* **1993**, *32*, 12522−12530.
(17) Puglisi, J. D.; Tan, R.; Calnan, B. J.; Frankel, A. D.; Williamson, J. R. *Science* **1992**, *257*, 76−80.
(18) Fritzsche, H.; Kan, L. S.; Ts'o, P. O. *Biochemistry* **1983**, *22*, 277−80.
(19) Deleted in proof.
(20) Cordingley, M. G.; Lafemina, R. L.; Callahan, P. L.; Condra, J. H.; Sardana, V. V.; Graham, D. J.; Nguyen, T. M.; Legrow, K.; Gotlib, L.; Schlabach, A. J.; Colonno, R. J. *Proc. Natl. Acad. Sci. U.S.A.* **1990**, *87*, 8985−8989.
(21) Brodsky, A. S.; Williamson, J. R. *J. Mol. Biol.* **1997**, *267*, 624−39.
(22) Roy, S.; Delling, U.; Chen, C. H.; Rosen, C. A.; Sonenberg, N. *Genes Dev.* **1990**, *4*, 1365−73.
(23) Weeks, K. M.; Crothers, D. M. *Cell* **1991**, *66*, 577−88.
(24) Boisbouvier, J.; Brutscher, B.; Pardi, A.; Marion, D.; Simorre, J. P. *J. Am. Chem. Soc.* **2000**, *122*, 6779−6780.
(25) Ippel, J. H.; Wijmenga, S. S.; deJong, R.; Heus, H. A.; Hilbers, C. W.; deVroom, E.; vanderMarel, G. A.; vanBoom, J. H. *Magn. Reson. Chem.* **1996**, *34*, S156−S176.
(26) Aboul-ela, F.; Karn, J.; Varani, G. *J. Mol. Biol.* **1995**, *253*, 313−32.
(27) Colvin, R. A.; White, S. W.; Garcia-Blanco, M. A.; Hoffman, D. W. *Biochemistry* **1993**, *32*, 1105−12.
(28) Jaeger, J. A.; Santalucia, J.; Tinoco, I. *Annu. Rev. Biochem.* **1993**, *62*, 255−287.

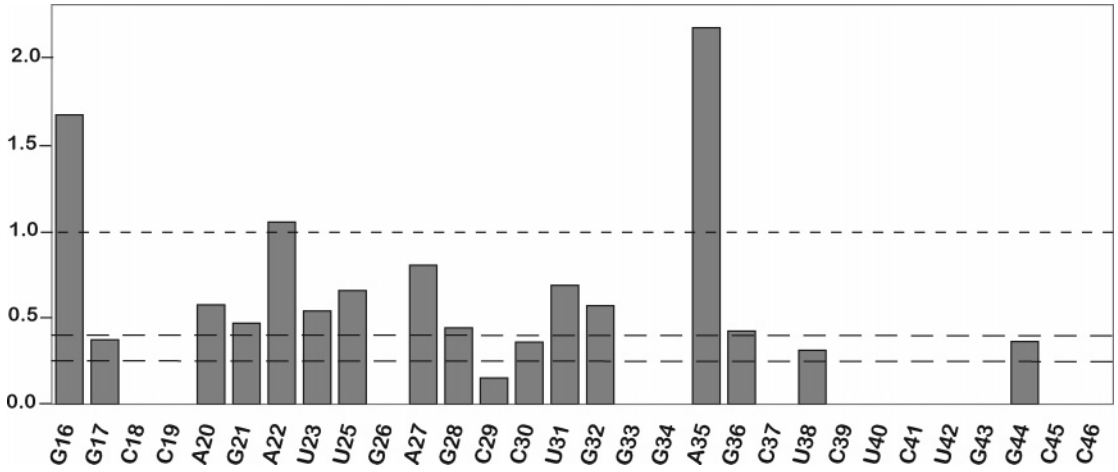

Figure 7. Histogram plot of signal-to-noise ratios (SN_{TACSY}/SN_{MQTR}). The region between the long dashed lines represents the expected level (0.25−0.4) in the absence of intermediate time scale exchange motions. The short dashed line shows the level (1.0) above which TACSY efficiency exceeds that of the MQ/TR counterpart. Residues with insufficient resolution to measure an accurate signal-to-noise ratio are omitted.

This confirms the existence of equilibrium between a conformation where A35 is stacked between G34 and G36 and a conformation where A35 is looped out. In agreement with these data, the largest sensitivity gain (2.2) is observed for residue A35. Biological data indicate that this site is in contact with both the Tat and the CycT1 protein in the process of HIV replication and is therefore of high functional relevance.[29−31] Also in this case, a regulatory role of the loop dynamics for the interactions of the TAR−RNA with the Tat/CycT1 complex can be hypothesized.

Intermediate time scale motions such as those described here for residues A22 and A35 are often identified for functionally relevant residues in RNA. Thus, the SHARP-TACSY pulse sequence, although less effective than established experiments for non-mobile residues, is a valuable tool for the assignment of resonances in crucial regions of biologically active RNA molecules.

Conclusions

We have proposed an alternative method for identifying base-to-sugar connectivity in RNA, based on selective heteronuclear planar mixing of the C6/8−N1/9−C1′ spin system. The SHARP-TACSY method requires a two-channel moderate power pulse train and can easily be implemented on most commercial spectrometers. Because of the nature of the mixing sequence, the transfer efficiency of nucleotides with considerable intermediate time scale motions in the base or sugar moieties exceeds that of conventional relaxation-optimized experiments.

We applied the SHARP-TACSY experiment to the 30-nt HIV-2 TAR, a long-chain polynucleotide featuring both canonical helical elements and noncanonical bulge and turn elements. A considerable sensitivity enhancement is observed for three nucleotides located at the end of the stem regions (G16, A22, and A35). These nucleotides have been found to undergo intermediate time scale motions either on the sugar or on the base. Two of them (A22 and A35) are located in functionally crucial regions.

These results underline the potential impact of this experiment on the NMR resonance assignment of nucleotides situated in the mobile sites of RNA, such as the crucial cofactor binding and enzymatic sites.

Acknowledgment. The authors thank Professors C. Griesinger and M. Reese for helpful discussions and C. Schwiegk for the synthesis of TAR RNA. This work is supported by the Deutsche Forschungsgemeinschaft (SFB416 to T.C.) and by the MPG.

Supporting Information Available: Reported chemical ranges and *J*-couplings of relevant nuclei used in this work (Table S1), shape parameters for 600−900 MHz fields (Table S2), and 2D H^bCNCH^s SHARP-TACSY of AGUC on TAR RNA (Figure S1). This material is available free of charge via the Internet at http://pubs.acs.org.

JA061424H

(29) Huq, I.; Rana, T. M. *Biochemistry* **1997**, *36*, 12592−9.
(30) Richter, S.; Cao, H.; Rana, T. M. *Biochemistry* **2002**, *41*, 6391−7.
(31) Richter, S.; Ping, Y. H.; Rana, T. M. *Proc. Natl. Acad. Sci. U.S.A.* **2002**, *99*, 7928−33.